

DESIGN AND ANALYSIS A CONTROLLER

FOR AUV PATH NAVIGATION SYSTEM

FAHMI AMIRUL BIN MOHAMMAD



Faculty of Mechanical Engineering

UNIVERSITI TEKNIKAL MELAYSIA MELAKA

MAY 2018

DECLARATION

I have declared that this project report entitled “Design and Analysis A Controller For AUV Path Navigation System” is the results of my own work except cited in references.

Signature :

Name of Supervisor :

Date :



APPROVAL

I hereby declare that I have read this project report and in my opinion this report is sufficient in terms of scope and quality for the award of the degree of Bachelor of Mechanical Engineering (Maintenance).

Signature

: 

Name of Supervisor

: Dr. MOHD KHARI

Date

: 4 / 7 / 19



اونيورسيتي تيكنيكل مليسيا ملاك

UNIVERSITI TEKNIKAL MALAYSIA MELAKA

DEDICATION

To my beloved parents Rosnah Bte A.Samad and Mohammad Bin Mohd Zain.



ABSTRACT

The uses of Autonomous Underwater Vehicle (AUV) is widely used in multiple field with each AUV have their own specific task given. AUV is designed to ease human work and extend the capability of human that are unable to do it such as operate for a long period of time in underwater and operate in a high-risk condition. For example, AUV been used in Oil and Gas industries to check underwater piping and it also been used in military as a valuable asset in surveying. AUV is not only been used in heavy industries but it is also being used for recreational purposes too. Most of the AUV have the same problem that hard to overcome which is to maintain its movement path to desire location. The water current is unpredictable this will make the AUV to drift away from its original path especially when the AUV operate in a deep ocean where the water current is really strong. Maintaining the AUV path is one of the big challenges in designing AUV so that it can operate efficiently with less disturbance towards its movement. If the AUV deviate away from its movement path this will causes the AUV to reach the desire location longer time as the AUV need to return to its original path and worst scenario the AUV might not reach its destination. Therefore, this project was carried out to design and analysis a controller for the AUV path navigation system. A PID controller was chose as the controller for the AUV. The mathematical modeling of the AUV is obtain and Simulink software were used to do the simulation of the AUV. The proportional gain, integral gain and derivative gain of the PID is study to understand the effect of each gain towards the speed and positioning of the AUV. Each PID gain effect the speed and positioning of the AUV differently and each gain is carefully selected to design a PID configuration that can improve the speed and position. The PID configuration undergoes fine adjustment to tweak some error. During the fine adjustment certain PID gain were changed to suit the configuration and the result is some gain manage to improve the speed and position.

ABSTRAK

Penggunaan *Autonomous Underwater Vehicle (AUV)* digunakan secara meluas di dalam pelbagai bidang di mana setiap *AUV* mempunyai ciri-ciri tertentu untuk melaksanakan tugas yang diberikan. *AUV* dicipta untuk memudahkan tugas manusia dan melaksanakan tugas yang diluar jangkauan manusia seperti beroperasi dibawah permukaan air bagi tempoh masa yang lama serta beroperasi dikawasan yang mempunyai risiko bahaya yang tinggi. Sebagai contoh, *AUV* digunakan di dalam bidang minyak dan gas untuk memeriksa paip di dasar lautan dan *AUV* juga digunakan dalam bidang ketenteraan sebagai asset penting untuk pemantauan. *AUV* juga bukan sahaja digunakan di dalam industri berat malahan digunakan sebagai tujuan rekreasi. Kebanyakan *AUV* mempunyai masalah yang sama yang sukar untuk diselesaikan iaitu untuk mengekalkan laluan pergerakan ke destinasi yang dikehendaki. Arus air sukar untuk diramal ia menyebabkan *AUV* mudah untuk menyimpang daripada laluan pergerakan yang asal terutama apabila beroperasi di laut dalam dimana arus air sangat kuat. Mengekalkan laluan pergerakan *AUV* adalah cabaran yang besar dalam mencipta *AUV* supaya *AUV* dapat beroperasi dalam kecekapan yang tinggi dengan sedikit gangguan terhadap pergerakan. Sekiranya *AUV* menyimpang daripada laluan pergerakan ini akan menyebabkan *AUV* untuk sampai ke destinasi yang dikehendaki dengan mengambil masa yang lama disebabkan *AUV* perlu membetulkan semula laluan pergerakannya dan bagi senario yang paling teruk *AUV* mungkin tidak akan sampai ke destinasi yang dikehendaki. Oleh sebab itu, projek ini dilaksanakan untuk mencipta dan menganalisa pengawal bagi pergerakan *AUV*. *PID* telah dipilih sebagai pegawai pergerakan *AUV*. Model matematik bagi *AUV* tersebut telah diperolehi dan perisian *Simulink* digunakan untuk membuat simulasi. 'Proportional Gain', 'Integral Gain', 'Derivative Gain' untuk *PID* tersebut telah di periksa dahulu untuk memahami bagaimana ianya mempengaruhi kelajuan dan pergerakan *AUV*. Setiap 'Gain' memberi kesan yang berlainan terhadap kelajuan dan pergerakan *AUV* dan setiap 'Gain' telah dipilih secara terperinci untuk digunakan sebagai konfigurasi *PID* bagi menambah baik kelajuan dan pergerakan *AUV*. Konfigurasi *PID* tersebut telah melalui proses pelarasan untuk membaiki ralat. Semasa proses pelarasan, 'Gain' pada *PID* telah diubah mengikut kesesuaian konfigurasi dan hasilnya sebahagian 'Gain' mampu memperbaiki kelajuan dan pergerakan.

ACKNOWLEDGEMENT

I would like to express my gratitude to my supervisor Dr. Mohd Khairi for helping me to finish this project. He always supports and guide me throughout this project were carried out. He also never hesitated in sharing his wide knowledge in AUV with me. When I facing some problems, he always sparks me with an idea to solve the problem and encourage me a lot to take every opportunity to learn about AUV. I am thankful for his patience and sincerity in helping me in this project.

Next, I would like to thank FKM Panther team for assisting and guide me especially during the Singapore Autonomous Underwater Challenge 2019. Hence, I would like to thank to my course mate for their moral support and suggestion.

Finally, I would like to express my appreciation to my family that always advise me and giving me word of wisdom so that I will never give up and keep optimistic.



CONTENT

CHAPTER CONTENT PAGE

SUPERVISOR'S DECLARATION	ii
TABLE OF CONTENT	viii
LIST OF FIGURES	ix
LIST OF ABBREVIATIONS	x
LIST OF SYMBOLS	xi
CHAPTER 1 INTRODUCTION	1
1.1 Background	1
1.2 Problem Statement	2
1.3 Objective	2
1.4 Scope of Project	3
CHAPTER 2 LITERATURE REVIEW	4
2.1 Autonomous Underwater Vehicle (AUV) Design	4
2.2 Autonomous Underwater Vehicle Controller	5
2.3 Comparison of PID and Fuzzy	6
2.4 Proportional Integral Derivative (PID)	7
CHAPTER 3 METHODOLOGY	9
3.1 Overview of Kinematics and Dynamic Model of AUV	9
3.2 Dynamic Model of AUV	10
3.2.1 Mass and Inertia Matrix	11

3.2.2	Coriolis and Centripetal Matrix	13
3.2.3	Hydrodynamic Damping Matrix	15
3.2.4	Gravitational and Buoyancy Matrix	16
3.2.5	Force and Torque Vector	17
3.3	Kinematics of AUV	18
3.3.1	Reference Frames	18
3.3.2	Euler Angles	19
3.3.3	State Space Representation of the AUV	20
3.4	PID Configuration Setting	21
3.4.1	PID Configuration Fine Adjustment	22
CHAPTER 4 RESULTS AND DISCUSSION		24
4.1	AUV Simulation	24
4.2	The Effect of K_p , K_i and K_d	27
4.3	The Configuration of the K_p , K_i , and K_d Gain	32
4.4	AUV Simulation Output Results	36
4.4.1	Position Output Data	37
4.4.2	Velocity Output Data	38
CHAPTER 5 CONCLUSION AND RECOMMENDATION		40
5.1	Conclusion	40
5.2	Recommendation	41
REFERENCE		42

LIST OF FIGURES

FIGURE PAGE	TITLE	
1.1	FKM team AUV	3
1.2	Flow chart	6
2.1	Blue Robotics automated underwater vehicle.	8
2.2	6 degree of freedom	9
3.1	AUV and B-frame reference frame	22
3.2	B-frame and W-frame	23
3.3	The stable and consistent oscillation of output loop	21
4.1	The Plant Model	24
4.2	Control Model	25
4.3	Full Model	26
4.4	Position error for reference model	27
4.5	Velocity error for reference model	27
4.6	Position data for PID $K_p = 7$, $K_i = 10$ $K_d = 4$	37
4.7	Position data for PID $K_p = 7$, $K_i = 7$ $K_d = 6$	37
4.8	Velocity data for PID $K_p = 7$, $K_i = 10$ $K_d = 4$	38
4.9	Velocity data for PID $K_p = 7$, $K_i = 7$ $K_d = 6$	39

LIST OF ABBREVIATIONS

AUV	Autonomous Underwater Vehicle
PID	Proportional Integral Derivative
DOF	Degree of Freedom
W-frame	World-fixed reference frame
B-frame	Body-fixed reference frame



LIST OF SYMBOLS

x_B	=	Surge B-frame
y_B	=	Sway B-frame
z_B	=	Heave B-frame
ϕ_B	=	Roll B-frame
θ_B	=	Pitch B-frame
ψ_B	=	Yaw B-frame
x	=	Surge W-frame
y	=	Sway W-frame
z	=	Heave W-frame
ϕ	=	Roll W-frame
θ	=	Pitch W-frame
ψ	=	Yaw W-frame
0_B	=	Origin of B-frame
0_W	=	Origin of W-frame
X	=	Degree of freedom of B-frame
η	=	Degree of freedom of W-frame
R^{BW}	=	Euler convention
v	=	Velocity vector of B-frame
$\dot{\eta}$	=	Velocity Vector of W-frame
τ	=	Force-torque vector of thruster input
v_B	=	Linear velocity of B-frame
ω_B	=	Angular velocity vector of B-frame.
v_W	=	Linear velocity of the W-frame
ω_W	=	Angular velocity of W-frame

$J(\eta)$	=	Coordinate transform matrix that brings the W-frame into alignment with B-frame
S	=	Sine
C	=	Cosine
T	=	Tangent
$M\dot{v}$	=	Mass and Inertia Matrix
$C(v)$	=	Coriolis and centripetal matrix
$D(v)$	=	Quadratic and linear drag matrix
$g(\eta)$	=	Gravitational and buoyancy matrix
τ	=	Force vector/ torque vector
M_{RB}	=	Mass of rigid body
M_A	=	Mass of added mass
m	=	Mass of the AUV
r_g	=	Center of gravity of AUV with respect of B-frame
I_B	=	AUV inertia tensor with respect to B-frame
C_{RB}	=	Coriolis rigid body term
C_A	=	Coriolis added mass term
$D_l(V)$	=	Linear drag matrix
$D_q(V)$	=	Quadratic drag matrix
X	=	Axial quadratic force
f_G	=	Gravitational force vector due to AUV weight
f_B	=	Buoyancy force vector caused by AUV buoyancy
L	=	Mapping matrix
U	=	Thrust Vector

CHAPTER 1

INTRODUCTION

1.1 Background

In this era where technology is becoming more and more sophisticated, AUV is not a something new anymore. AUV stand for autonomous underwater vehicle are untethered unmanned maritime robotic platforms. AUV is one of the categories of unmanned underwater vehicle (UUV) while the other one is remotely operated underwater vehicle, ROV. ROV have its own limitation where AUV can handle it. The need for a communication tether and a control platform for ROV have limited the use of ROV and also its capabilities due to the depth of water. This is where AUV become in handy because AUV doesn't need any human to operate it because AUV will think by itself in order to execute given mission. During 1957, the first AUV was developed by Stan Murphy, Bob Francois and later on by Terry Ewart at Applied Physics Laboratory at University of Washington. There're wide range of AUV application such as for commercial use, research, hobby, air crash investigation, and also military application.

1.2 Problem Statement

An autonomous underwater vehicle (AUV) is the machine that can operate underwater autonomously without the help from the operator. AUV is widely used in many field such as for maintenance of underwater structure like oil rig and bridge, detecting and mapping submerged wreck and obstruction that are potentially dangerous for commercial and recreational vessels navigation. Since the MH370 tragedy AUV became well known around the globe in aiding the search of the crash airplane. The usage of AUV is very challenging especially for its navigation. The ocean current is unpredictable thus the AUV can easily drift away without a proper navigation system. The main problem with AUV is to create a navigation system that can ensure the AUV move to the desired location accurately. Nowadays, researcher is still struggling in creating the almost perfect navigation system for AUV. This project is focus on creating the proper navigation system for the PID by using PID as its controller.

1.3 Objective

The objective of this project is as follow:

1. To design and analysis the controller for AUV to make it move according to desired path.

1.4 Scope of Project

The scopes of this project are:

1. The controller is for AUV developed by FKM team as shown below

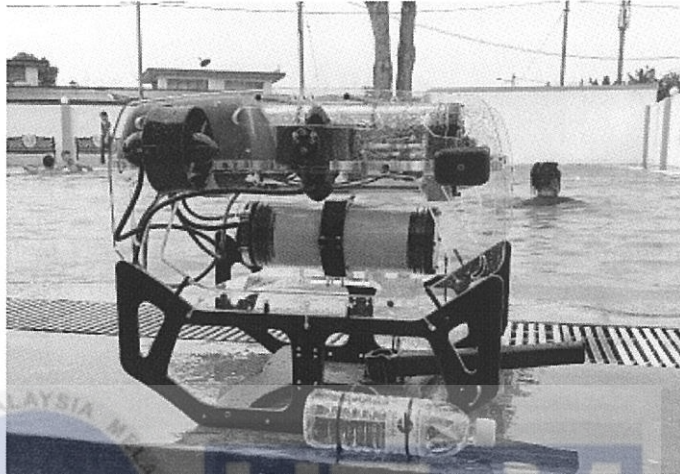


Figure 2.1 FKM team AUV.

2. The dimension of the AUV is not exceed $140 \times 100 \times 100 \text{ cm}$ and less than 50kg in mass.
3. The controller is design to improve the positioning and speed of AUV.
4. Simulink software is used to simulate the AUV in the real world.
5. The simulation is only for surge degree of freedom only.

CHAPTER 2

LITERATURE REVIEW

2.1 Autonomous Underwater Vehicle (AUV) Design

Designing an AUV has several stages that generally can be divided into two stages which are designing the mechanical structure and the other one is the development of internal and external electrical design. It's vital to have a proper knowledge when designing AUV especially about the concept, theory, and physical law of AUV while it's underwater in a vary condition. A proper mechanical and electrical design play an important role in order to determine the successful of the AUV because it will aid the AUV navigation. The structure and design aspect that need to be focus are such as hull design, propulsion, electric power, and submerging. After the AUV is well designed a controller is added to navigate and ensure the AUV move according to the trajectories and also reached the desired location without overshoot. This controller act like a brain that instruct the AUV to move with the helped of the mechanical and electrical structure of the AUV so if the AUV have any defect with its design then the brain can't operate efficiently. Figure 2.1 shows commercial AUV that is customizable.

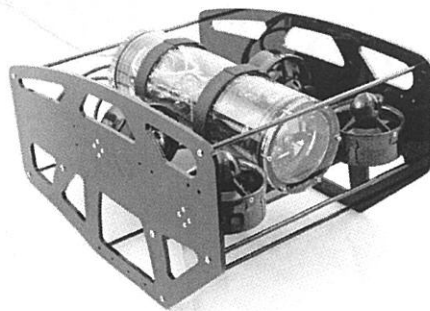


Figure 2.2 Blue Robotics automated underwater vehicle.

2.2 AUV Controller

There're many types of controller being used in AUV to help its navigation such as PID, Fuzzy, Feed Forward Controller and Velocity Feedback Controller but the most commonly used are Fuzzy and PID controller. The controller selection depends on the characteristic of the AUV because not every controller suitable for every AUV this is due to each AUV have different specification and job scope. Every AUV doesn't limited to only one controller only it can have more than one controller as stated by the author their AUV have 3 controllers onboard and it's also not a compulsory to have more than one controller. The AUV that have many controllers onboard, each of the controller will have different output such as there will be controller that controlling the motion axis of the AUV and there will be controller that will control the speed of the AUV. Whereas, the AUV that only have one controller, the controller will control both of the motion axis of AUV and the speed of the AUV. In designing AUV one must consider the motion axis which is 6 degree of freedom (DOF) as shown in figure 2.2. The controller will take all of the 6 DOF into calculation to come out with a suitable equation of motion but this is complex. Hence, in order to make the AUV less complicated the controller only responsible to 3 Degree of Freedom (DOF) instead of 6 DOF because If the AUV is symmetry the DOF can be decoupled into 3 DOF which are Surge, Heave and Yaw degrees of freedom.

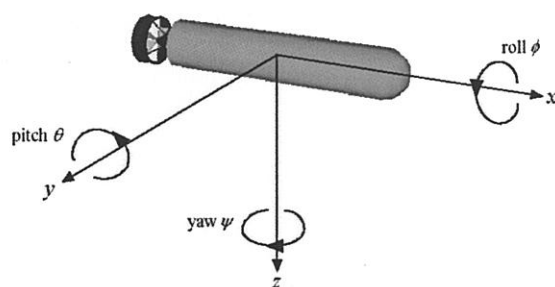


Figure 2.3 shows 6 degree of freedom.

2.3 Comparison of PID and Fuzzy

The advantages of PID controller is it provide of simple, clear, practical parameter of stable and reliable while it disadvantage is mathematical model need to be accurately establish. Fuzzy doesn't need an accurate mathematical model resulting the limitation of sensitivity and stability of the AUV. In general, Fuzzy logic controller tuning process is mainly by trial-and-error while for PID the tuning process are by tuning the value of the system parameter. In term of rise time, and overshoot PID give a better performance compare to Fuzzy.



2.4 Proportional Integral Derivative (PID)

As mention in 2.2 AUV Controller the controller that are mostly been used are PID and Fuzzy controller. Matlab/Simulink can run both of the controller but they have different tuning process and the way they work to get an output is much different. PID means Proportional-Integral-Derivative (PID) where it is a mechanism that have a control loop feedback. The way the PID work is by continuously calculates the difference value between the setpoint to the system and the measured process variable. The difference value is known as error value $e(t)$ which then will be corrected based on the proportional, integral and derivative as the PID name itself. The PID can be expressed mathematically as

$$u(t) = K_p e + K_i \int e + K_d \frac{de}{dt}$$

Where:

$u(t)$: Output of the system

K_p : Proportional gain

K_i : Integral gain

K_d : Derivative gain

e : Error between setpoint and the measured process variable

$\int e$: Summation error of steady state error

$\frac{de}{dt}$: Rate of change of error

K_p will make sure the error is small and if there is any deviation from the setpoint then it will alter the system to closer to the setpoint but it doesn't have much effect to counter steady-state error.

K_i is the gain that will reduce or eliminate the steady-state error due to the uniform or slow changing imbalance or disturbance towards the system. Overtime the steady-state error will accumulate and become larger hence, K_i create a required request for actuation to eliminate it.

K_d act as a damper for the system. It's used to reduce the rate of change of the state in order to avoid from overshoot and oscillations. Thus, K_p and K_i can be larger and have more control of the system. Figure 2.3 illustrates basic close-loop depth control using PID controller.

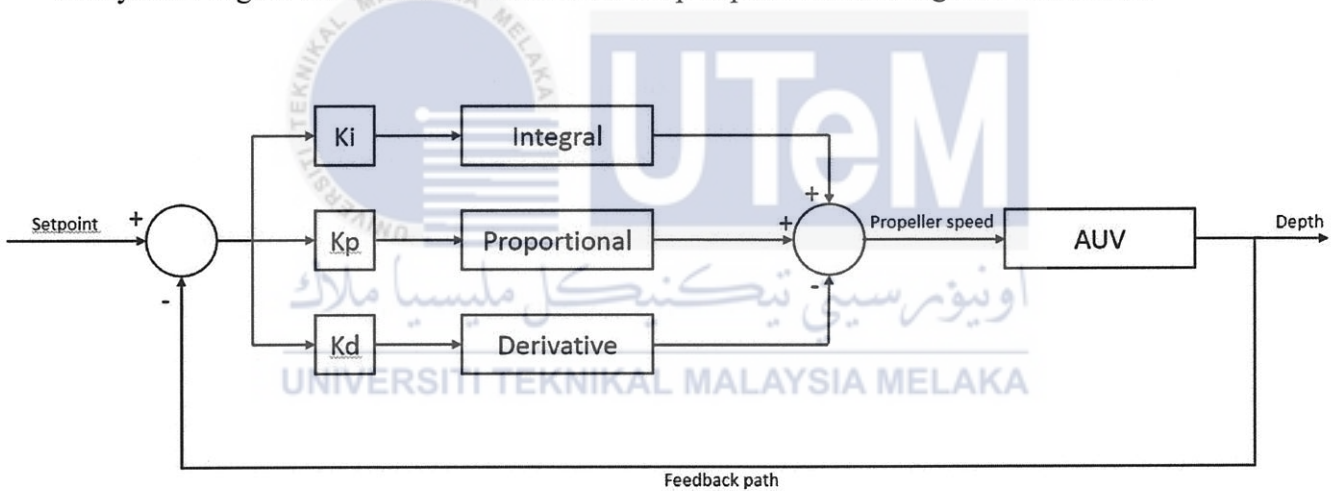


Figure 2.3 PID controller used for depth control.

CHAPTER 3

METHODOLOGY

3.1 Overview of Kinematic and Dynamic Model of AUV

Controlling an AUV underwater is intricate due to the complex and nonlinear force that acting upon the AUV while working underwater. The example of the forces are environmental disturbances, thruster force, gravity and buoyance force, Coriolis and centripetal force, lift forces, damping and hydrodynamic drag.

Dynamic Model of AUV will be discuss on next section which will describe about the hydrodynamic damping, gravitation and buoyance force, mass and inertia, and Coriolis and centripetal force. The afterwards section, discuss about Kinematic of the AUV where state space representation, Euler angles, and reference frame explained.

UNIVERSITI TEKNIKAL MALAYSIA MELAKA

3.2 Dynamic Model of AUV

Newton Euler equation of a rigid body in fluid is derived to get the Dynamic Model of the AUV (W & C, 2001). Later, the equation is able to do simulation and to formulate control algorithm for the AUV. The dynamic model is as below and it's not considering environmental disturbance

$$M\dot{v} + C(v)v + D(v)v + g(\eta) = \tau \quad (3.1)$$

Where,

$M = M_{RB} + M_A$: Mass and inertia matrix.

$C(V) = C_{RB}(V) + C_A$: Coriolis and centripetal matrix.

$D(V) = D_q(V) + D_l(V)$: Quadratic and linear drag matrix.

$g(\eta)$: Gravitational and buoyancy matrix.

τ : Force vector/ torque vector.

3.2.1 Mass and Inertia Matrix

$$M = M_{RB} + M_A \quad (3.2)$$

Mass and Inertia matrix is a submission of rigid body, M_{RB} and added mass, M_A . Added mass is a part of hydrodynamic force and moment. It's also known as pressured induced force and/or moment which is the result of AUV body force motion.

The expand equation of rigid body, $M_{RB}\dot{V}$ from (3.1) is

$$M_{RB}\dot{V} = \begin{bmatrix} m\dot{v}_B + m\dot{\omega}_B \times r_g \\ I_B\dot{\omega}_B + mr_G \times \dot{v}_B \end{bmatrix} \quad (3.3)$$

Where,

m : Mass of the AUV.

r_g : Center of gravity of AUV with respect of B-frame.

$$r_g = [x_G \quad y_G \quad z_G]^T$$

I_B : AUV inertia tensor with respect to B-frame

$$I_B = \begin{bmatrix} I_{xx} & -I_{xy} & -I_{xz} \\ -I_{yx} & I_{yy} & -I_{yz} \\ -I_{zx} & -I_{zy} & I_{zz} \end{bmatrix} \quad (3.4)$$

$$I_{xx} = \int (y^2 + z^2) dm$$

$$I_{xy} = I_{yx} = -\int (xy) dm$$

$$I_{yy} = \int (x^2 + z^2) dm$$

$$I_{yz} = I_{zy} = -\int (yz) dm$$

$$I_{zz} = \int (x^2 + y^2) dm$$

$$I_{xz} = I_{zx} = -\int (xz) dm$$

The AUV operate at relative low speed thus it can be assumed to be symmetric even though the x-y plane of the AUV is not while y-z plane is almost symmetric and x-z plane is symmetric. Hence, the origin of the B-frame is located at the center of gravity of AUV, i.e. $r_g = [0 \ 0 \ 0]^T$, then the equation of rigid body mass, M_{RB} is

$$M_{RB} = \begin{bmatrix} m & 0 & 0 & 0 & 0 & 0 \\ 0 & m & 0 & 0 & 0 & 0 \\ 0 & 0 & m & 0 & 0 & 0 \\ 0 & 0 & 0 & I_{xx} & 0 & 0 \\ 0 & 0 & 0 & 0 & I_{yy} & 0 \\ 0 & 0 & 0 & 0 & 0 & I_{zz} \end{bmatrix} \quad (3.5)$$

The design shape of the AUV will determine the added mass matrix terms. Previously the AUV is assumed to be symmetric and B-frame origin located at the center of gravity, then the hydrodynamic added mass is,

$$M_A = \begin{bmatrix} X_{\dot{u}} & 0 & 0 & 0 & 0 & 0 \\ 0 & Y_{\dot{v}} & 0 & 0 & 0 & 0 \\ 0 & 0 & Z_{\dot{w}} & 0 & 0 & 0 \\ 0 & 0 & 0 & K_{\dot{p}} & 0 & 0 \\ 0 & 0 & 0 & 0 & M_{\dot{q}} & 0 \\ 0 & 0 & 0 & 0 & 0 & N_{\dot{r}} \end{bmatrix} \quad (3.6)$$

If the AUV is fully submerged the parameter of added mass is consider as constant.

3.2.2 Coriolis and Centripetal Matrix

$$C(v) = C_{RB}(v)v + C_A(v) \quad (3.7)$$

The Coriolis force is an inertial force that act to the left of the direction of a body motion that rotate clockwise and it will act to the right of the direction of body motion that rotate counterclockwise. Centripetal force is a total force that acting on an object that will ensure the object to move along circular path. The Coriolis and Centripetal Matrix rigid body term, C_{RB} is

$$C_{RB}(v)v = \begin{bmatrix} m\omega_B \times v_B + m\omega_B \times (\omega_B \times r_g) \\ \omega_B \times (I_B\omega_B) + mr_G \times (\omega_B \times v_B) \end{bmatrix} \quad (3.8)$$

Where,

m : AUV mass
 r_g : Center of gravity of AUV with respect of B-frame.

$$r_g = [x_G \quad y_G \quad z_G]^T$$

I_B : AUV inertia tensor with respect to B-frame (3.4)

ω_B : Angular velocity vector of B-frame.

The rigid body term is

$$C_{RB}(v) = \begin{bmatrix} 0 & 0 & 0 & 0 & mw & -mv \\ 0 & 0 & 0 & -mw & 0 & mu \\ 0 & 0 & 0 & mv & -mu & 0 \\ 0 & mw & -mv & 0 & I_{zz}r & I_{yy}q \\ -mw & 0 & mu & -I_{zz}r & 0 & I_{xx}P \\ mv & -mu & 0 & I_{yy}q & -I_{xx}P & 0 \end{bmatrix} \quad (3.9)$$

The AUV hydrodynamic added mass Coriolis-like matrix is

$$C_A(v) = \begin{bmatrix} 0 & 0 & 0 & 0 & -\alpha_3(v) & \alpha_2(v) \\ 0 & 0 & 0 & \alpha_3(v) & 0 & -\alpha_1(v) \\ 0 & 0 & 0 & -\alpha_2(v) & \alpha_1(v) & 0 \\ 0 & -\alpha_3(v) & \alpha_2(v) & 0 & -\beta_3(v) & \beta_2(v) \\ \alpha_3(v) & 0 & -\alpha_1(v) & \beta_3(v) & 0 & -\beta_1(v) \\ -\alpha_2(v) & \alpha_1(v) & 0 & -\beta_2(v) & \beta_1(v) & 0 \end{bmatrix}$$

Where,

$$\alpha_1(v) = X_{\dot{u}}u + Y_{\dot{v}}v + X_{\dot{w}}w + X_{\dot{p}}p + X_{\dot{q}}q + X_{\dot{r}}r$$

$$\alpha_2(v) = X_{\dot{v}}u + Y_{\dot{v}}v + Y_{\dot{w}}w + Y_{\dot{p}}p + Y_{\dot{q}}q + Y_{\dot{r}}r$$

$$\alpha_3(v) = X_{\dot{w}}u + Y_{\dot{w}}v + Z_{\dot{w}}w + Z_{\dot{p}}p + Z_{\dot{q}}q + Z_{\dot{r}}r$$

$$\beta_1(v) = X_{\dot{p}}u + Y_{\dot{p}}v + Z_{\dot{p}}w + K_{\dot{p}}p + K_{\dot{q}}q + K_{\dot{r}}r$$

$$\beta_2(v) = X_{\dot{q}}u + Y_{\dot{q}}v + Z_{\dot{q}}w + K_{\dot{q}}p + M_{\dot{q}}q + M_{\dot{r}}r$$

$$\beta_3(v) = X_{\dot{r}}u + Y_{\dot{r}}v + Z_{\dot{r}}w + K_{\dot{r}}p + M_{\dot{r}}q + N_{\dot{r}}r$$

UNIVERSITI TEKNIKAL MALAYSIA MELAKA

3.2.3 Hydrodynamic Damping Matrix

$$D(V) = D_q(V) + D_l(V)$$

The AUV hydrodynamic damping consist of drag and lift forces while underwater. However, the lift forces can be neglect due to the speed of the AUV is operates at slow speed. The drag force can be divided into linear, $D_l(V)$ and quadratic, $D_q(V)$. The AUV is assumed to be symmetry so the equation is

$$D_l(V) = \begin{bmatrix} X_u & 0 & 0 & 0 & 0 & 0 \\ 0 & Y_v & 0 & 0 & 0 & 0 \\ 0 & 0 & Z_w & 0 & 0 & 0 \\ 0 & 0 & 0 & K_p & 0 & 0 \\ 0 & 0 & 0 & 0 & K_q & 0 \\ 0 & 0 & 0 & 0 & 0 & N_r \end{bmatrix} \quad (3.10)$$

The AUV axial quadratic drag force is modeled with

$$X = - \left(\frac{1}{2} \rho C_d A_f \right) u |u| = X_{u|u} u |u| \quad (3.11)$$

Where,

$$X_{u|u} = \frac{\partial X}{\partial (u|u)} = -\frac{1}{2} \rho C_d A_f$$

The quadratic drag matrix is derive from the matrix notation of (3.11) is

$$D_q(V) = \begin{bmatrix} X_{u|u}|u| & 0 & 0 & 0 & 0 & 0 \\ 0 & Y_{v|v}|v| & 0 & 0 & 0 & 0 \\ 0 & 0 & Z_{w|w}|w| & 0 & 0 & 0 \\ 0 & 0 & 0 & K_{p|p}|p| & 0 & 0 \\ 0 & 0 & 0 & 0 & K_{q|q}|q| & 0 \\ 0 & 0 & 0 & 0 & 0 & N_{r|r}|r| \end{bmatrix} \quad (3.12)$$

3.2.4 Gravitational and Buoyancy Matrix

$$g(\eta) = \begin{bmatrix} f_B + f_G \\ r_B \times f_B + f_G \times f_G \end{bmatrix} \quad (3.13)$$

Where,

f_G : Gravitational force vector due to AUV weight.

$$f_G = R^{BW^{-1}}(v_w)[0 \ 0 \ W]^T, \quad W = mg \quad (3.14)$$

f_B : Buoyancy force vector caused by AUV buoyancy.

$$f_B = R^{BW^{-1}}(v_w)[0 \ 0 \ -B]^T, \quad B = \rho g \nabla \quad (3.15)$$

$g = 9.81 \text{ m/s}^2$, $\rho = \text{fluid density}$,

$\nabla = \text{volume of fluid displaced by the AUV}$

r_G : AUV center of gravity.

$$r_G = [x_B \ y_B \ z_B]^T$$

r_B : AUV center of buoyancy.

$$r_B = [x_B \ y_B \ z_B]^T$$

The equation of (3.21) and (3.22) will be substitute into (3.20) to get equation below

$$g(\eta) = \begin{bmatrix} (W - B) \sin(\theta) \\ -(W - B) \cos(\theta) \sin(\phi) \\ -(W - B) \cos(\theta) \cos(\phi) \\ -(y_g W - y_b B) \cos(\theta) \cos(\phi) + (z_g W - z_b B) \cos(\theta) \sin(\phi) \\ (z_g W - z_b B) \sin(\theta) + (x_g W - x_b B) \cos(\theta) \cos(\phi) \\ -(x_g W - x_b B) \cos(\theta) \sin(\phi) - (y_g W - y_b B) \sin(\theta) \end{bmatrix} \quad (3.16)$$

3.2.5 Force and Torque Vector

$$\tau = LU \quad (3.17)$$

The AUV have thrust force and torque force that coming from the horizontal thruster and vertical thruster that will allow the AUV to move in surge, heave, roll, pitch and yaw directions. The force and torque vector is defined as above (3.17).

Where,

L : Mapping matrix that indicates the direction of the force (surge and heave DOF) and the direction and arm of the torque (roll, pitch and yaw DOF).

$$L = \begin{bmatrix} 1 & 1 & 0 & 0 & 0 & 0 \\ 0 & 0 & 0 & 0 & 0 & 0 \\ 0 & 0 & 1 & 1 & 1 & 1 \\ 0 & 0 & -l_1 & -l_2 & -l_1 & -l_2 \\ -l_3 & -l_3 & -l_6 & -l_6 & -l_5 & -l_5 \\ -l_1 & -l_2 & 0 & 0 & 0 & 0 \end{bmatrix} \quad (3.18)$$

U : Thrust vector that indicates each of trolling motor thrust.

$$U = [T_1 \ T_2 \ T_3 \ T_4 \ T_5 \ T_6] \quad (3.19)$$

3.3 Kinematics of AUV

In the Kinematics of AUV subsection the reference frames, the use of Euler angles and the state space representation of the AUV will be discussed in details. Figure below illustrates the relationship between AUV and B-frame reference frame.

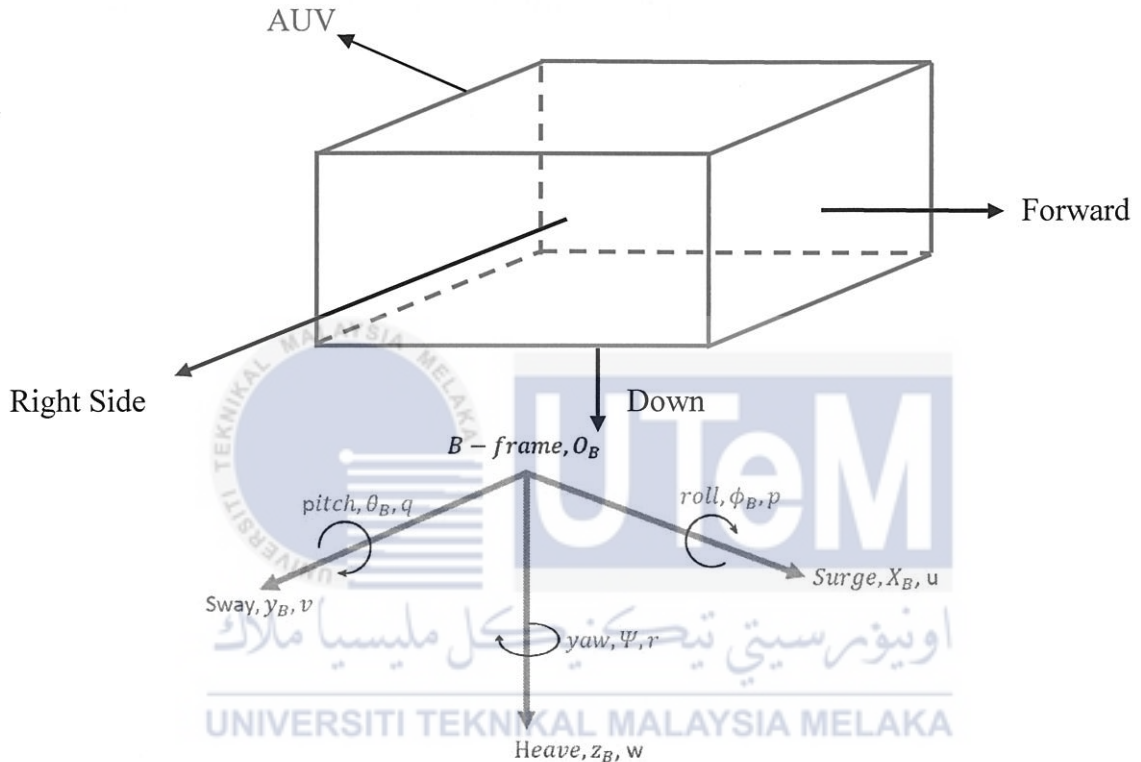


Figure 3.1 AUV and B-frame reference frame.

3.3.1 Reference Frames

World-fixed reference frame (W) and a body-fixed frame (B) are two reference frames that will be used for the AUV as illustrated in figure (3.20). The B-frame will be set to the AUV body while W-frame is set to the world where its location can be anywhere on the earth. Hence, the orientation, velocity, and acceleration of the AUV can be determined with respect to the world and AUV coordinates. The x-axis of B-frame is pointing to the forward while y-axis and z-axis are pointing to the right and vertically down respectively. The W-frame x-axis is facing to the north,

y-axis facing east and z-axis facing to the center of the earth. The B-Frame degree of freedom are *Surge*, x_B , *Sway*, y_B , *Heave*, z_B , *Roll*, ϕ_B , *Pitch*, θ_B , and *yaw*, ψ_B . The B-frame and W-frame origin are defined as O_B and O_w respectively and all of the DOF for both reference frame is as below in a vector form

$$X = [\textit{surge} \ \textit{sway} \ \textit{heave} \ \textit{roll} \ \textit{pitch} \ \textit{yaw}]^T \quad (3.20)$$

$$[x_B \ y_B \ z_B \ \phi_B \ \theta_B \ \psi_B]^T$$

$$\eta = [x \ y \ z \ \varphi \ \theta \ \psi]^T \quad (3.21)$$

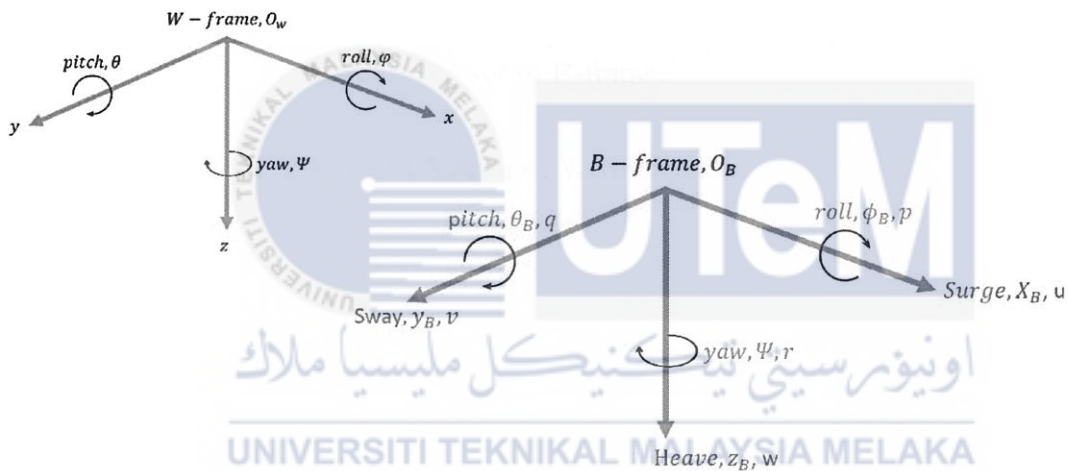


Figure 3.2 shows B-frame and W-frame.

3.3.2 Euler Angles

In order to characterize the orientation from AUV to the world the Euler convention is required. The system coordinate can be orientate to another system coordinate such as B-frame to W-frame it will involve an array of three rotation that is z - y - x . Firstly, the B-frame rotate at z -axis, ψ_B then at y -axis *pitch*, θ_B and lastly at x -axis *roll*, ϕ_B . Figure (3.1) shows the B-frame orientation with respect to the W-frame in a form rotation matrix

$$R^{BW}(\varphi, \theta, \psi) = R_z(\psi)R_y(\theta)R_x(\varphi) \quad (3.22)$$

3.3.3 Vector Representation of the AUV

In order to analyze and have a compact way to model AUV Vector Representation can be used. The equation X (3.20) and η (3.21) are included in the vector notation.

$$v = [\dot{x}_B \ \dot{y}_B \ \dot{z}_B \ \dot{\phi}_B \ \dot{\theta}_B \ \dot{\psi}_B]^T = [u \ v \ w \ p \ q \ r]^T \quad (3.23)$$

$$\dot{\eta} = [\dot{x} \ \dot{y} \ \dot{z} \ \dot{\phi} \ \dot{\theta} \ \dot{\psi}]^T$$

$$\tau = [\tau_u \ \tau_v \ \tau_w \ \tau_\phi \ \tau_\theta \ \tau_\psi]^T$$

Where,

v : Velocity vector of B-frame.

$\dot{\eta}$: Velocity Vector of W-frame.

τ : Force-torque vector of thruster input.

3.4 PID Configuration Setting

The PID gains have different effect towards the AUV. Thus, for each PID gains it is required to study the effect pattern of the gains. In order to study the effect of the PID gains, Ziegler-Nichols method is used as the baseline of the PID configuration.

Ziegler-Nichols method was developed by John G. Ziegler and Nathaniel B. Nichols. First, the Integral gain, K_i and Derivative gains, K_d is set to zero. Then the Proportional gain is increase from one until it reaches the ultimate gain, K_u . The ultimate gain, K_u is where the output loop has stable and consistent oscillation as shown in figure 3.3 below.

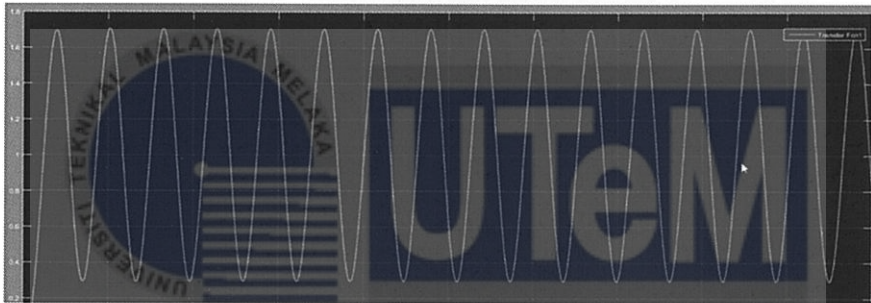


Figure 3.3 shows the stable and consistent oscillation of output loop.

After the ultimate gain, K_u is achieved, the oscillation period, T_u for which the time required for one complete oscillation is recorded. The ultimate gain, K_u and oscillation period, T_u are used in the formula (classis PID) as shown in table 3.1 below to find the PID configuration.

Table 3.1 shows the Ziegler-Nichols method formula.

Control Type	K_p	T_i	T_d	K_i	K_d
P	$0.5K_u$	–	–	–	–
PI	$0.45K_u$	$T_u/1.2$	–	$0.54K_u/T_u$	–
PD	$0.8K_u$	–	$T_u/8$	–	$K_u T_u/10$
classic PID ^[2]	$0.6K_u$	$T_u/2$	$T_u/8$	$1.2K_u/T_u$	$3K_u T_u/40$
Pessen Integral Rule ^[2]	$7K_u/10$	$2T_u/5$	$3T_u/20$	$1.75K_u/T_u$	$21K_u T_u/200$
some overshoot ^[2]	$K_u/3$	$T_u/2$	$T_u/3$	$0.666K_u/T_u$	$K_u T_u/9$
no overshoot ^[2]	$K_u/5$	$T_u/2$	$T_u/3$	$(2/5)K_u/T_u$	$K_u T_u/15$

The PID configuration of the Ziegler-Nichols method is adjusted starting with the proportional gain, K_p where it is increased until the pattern of the gains towards the position and velocity are clearly visible while the integral gain, K_i and derivative gain, K_d are constant.

Next, based on the study of the proportional gain, K_p , previously, the value of K_p that has lowest position and velocity error is choose to set as a new K_p to study the integral gain, K_i . Same as previous step, the K_i will slowly increase where the K_d value is constant and K_p value is set to the newest value as stated above.

Finally, to study the effect of derivative gain, K_d the K_d value is increased until the pattern of K_d towards the position and velocity error are visible. For the K_p and K_i value they are set to the lowest position and velocity error based on their studied respectively.

All of the PID gains pattern are studied, and each gains value that has lowest position error will be choose to form a new PID configuration that will undergo fine adjustment in order to reduce the error of position and velocity.

3.4.1 PID Configuration Fine Adjustment

The new PID configuration are required to undergo fine adjustment to optimize the configuration. For fine adjustment, only a single gain will be change for example for K_p fine adjustment the value of K_p only will be change while K_i and K_d are constant. This step is same as for the K_i and K_d fine adjustment.

K_p fine adjustment is done by first choosing the value that has lowest position error. The value is set and the simulation is run. If the PID configuration fail to improve the error of the position and velocity then the K_p value is changed to the K_p value that has second lowest

position error. If the configuration failed too then K_p is changed to the next lowest position error value this step is repeated until position error is unlikely to improve.

The K_i and K_p fine adjustment are same as the K_p fine adjustment where only the gain that need to undergo fine adjustment is changed while the other two gains are constant.

By doing the fine adjustment for each gain, the error of position is improved where each fine adjustment yields different results. Each PID gains fine adjustment, has different PID configuration. The PID configuration that successfully improved the position error by larger percentage are the best PID configuration.



The Plant model input signals are the thrust (T) and plant velocity (xdot) while the output signals is the AUV real-time position (x).

The trajectory model acceleration signals are defined by a cosine function as shown in table 4.1. The frequency and maximum amplitude of the signal are 0.3 Hz and 0.1 m/s^2 . The velocity and position reference signals are obtained through the integration of the cosine function twice.

Table 4.1 Trajectory model data

Function	$\ddot{r} = 0.1\cos(0.6\pi t)$
Max (r)	2.22 m
Max (\dot{r})	0.33 m/s
Max (\ddot{r})	0.10 m/s^2

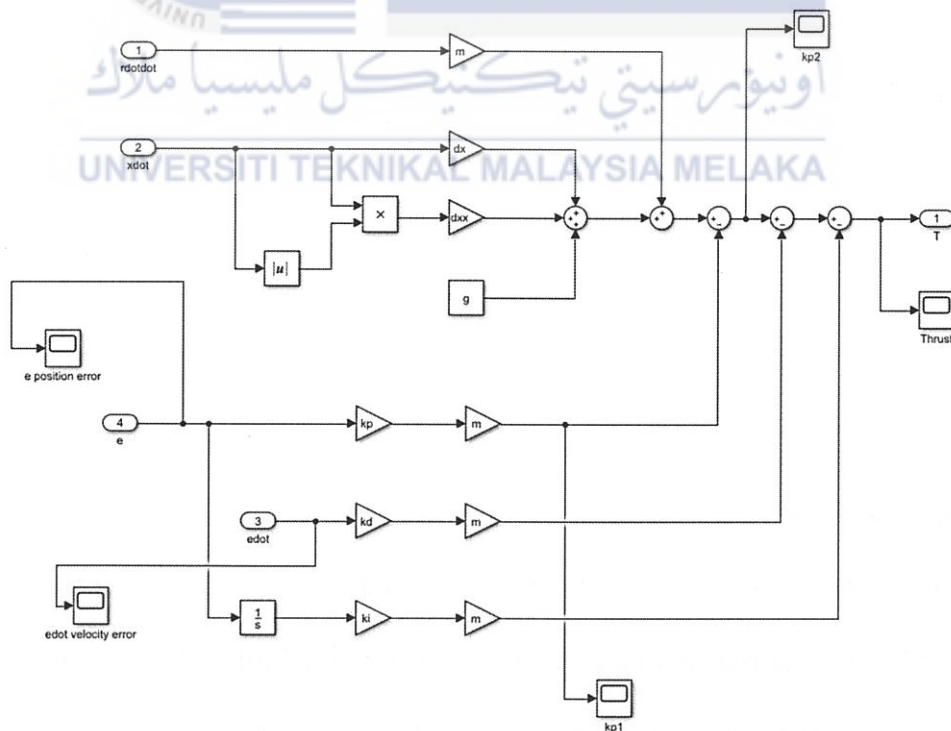


Figure 4.2 Control Model

The control model has an input signals of reference acceleration (\ddot{r}), velocity (\dot{x}), velocity error (\dot{e}) and position error (e). The output signal is thrust (T). The PID gain (K_p , K_i , K_d) of the AUV is adjusted in the control model.

After the plant model, trajectory model and control model are designed and no error occurred during compiling then they are connected to each another in the Simulink as shown in the figure 4.3 below.

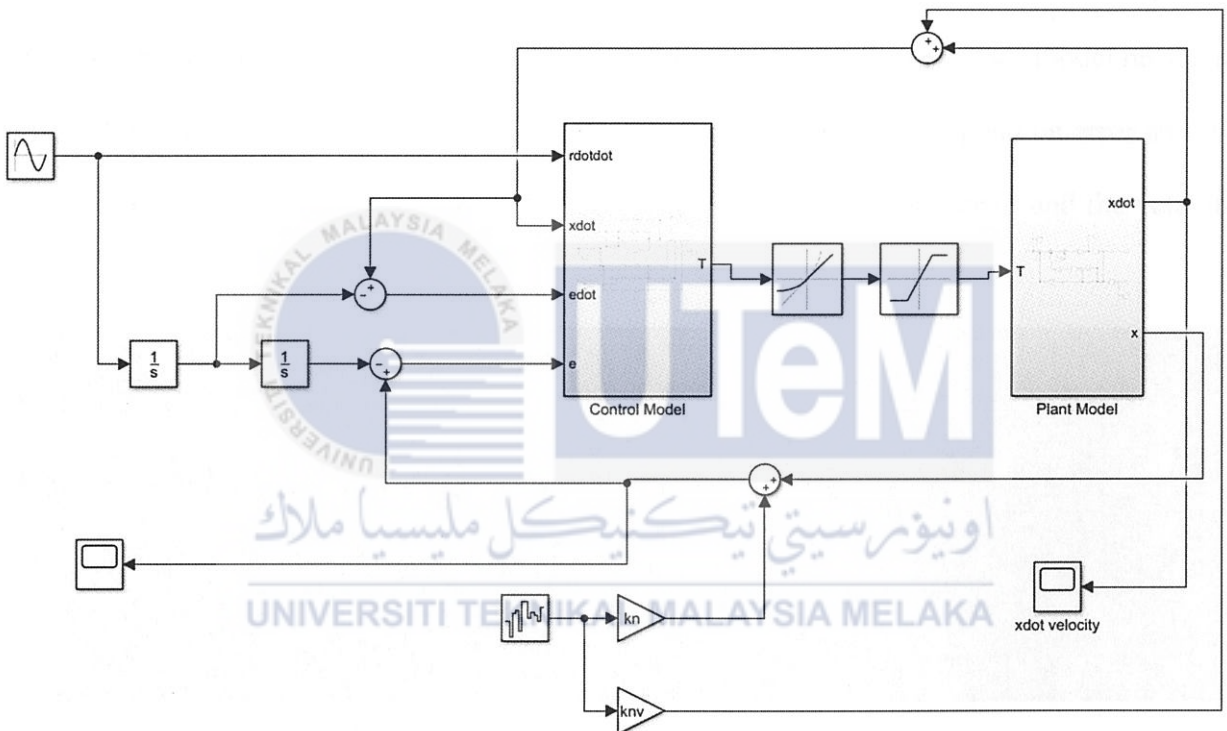


Figure 4.3 Full model which control model, plant model and trajectory model connected to each other.

White noise is added in order to determine the plant position and velocity because in reality the level of noise will be measured to determine the current position and velocity of the AUV. In the simulation a rate limiter is added that connected to the thrust output. This is due to the trolling motor will not capable to immediately switch the direction of the AUV thrust from forward (positive value) and backward (negative value) because of the inertia for example, from

-30N (backward) to +30N (forward). Thus, the rate limiter will ensure that the rate of change of the thrust is not exceed 100 N in one second for each trolling motor. In reality every AUV thruster have their own capability to give an output and have their own limit thus saturation is added to set every thruster to give 50 N of thrust.

4.2 The Effect of K_p , K_i and K_d

Based on the reference model results it will be used as the benchmark for this project results. The result yields from this project will be compared with the reference model results to check for any improvement or error. This project will be comparing the position error and the velocity error of the AUV simulation. Figure below shows the position error and the velocity error of the reference model.

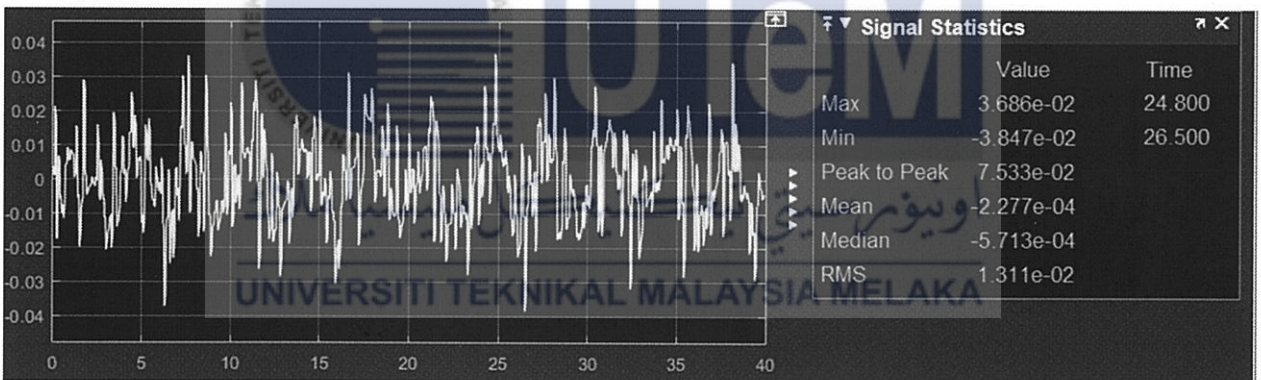


Figure 4.4 Position error for reference model.

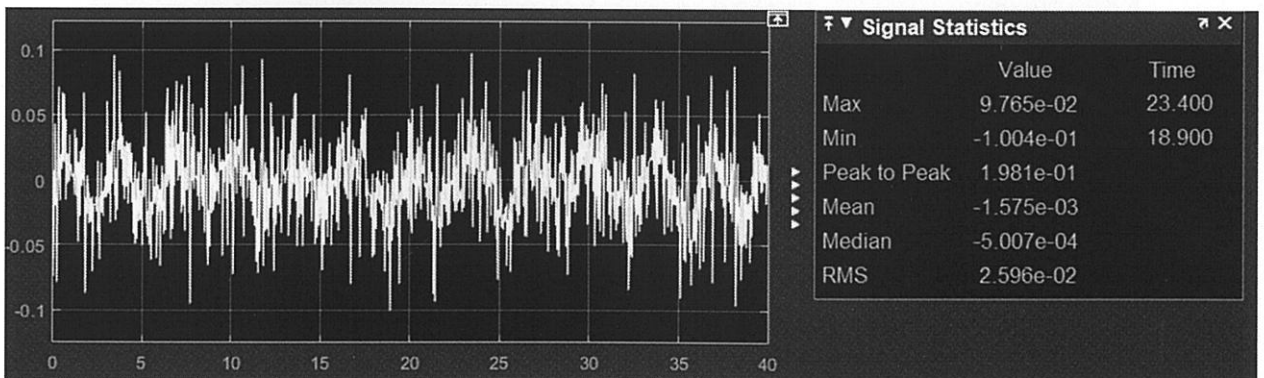


Figure 4.5 Velocity error for reference model.

The y-axis and x-axis for position error graph are meter and second respectively. The velocity error graph y-axis is meter per second while the x-axis is second. The simulation is running for 40 second that is why both of the graph x-axis only running until 40 seconds.

The mean for the position error graph is -0.0417m while the mean for the velocity error graph is -0.0784 m/s. Both graphs are running with the same gain number for the PID which are the proportional gain K_p , integral gain K_i , and derivative gain K_d are 9, 10, and 6 respectively. This project will find the best possible value for the K_p , K_i and K_d gain to minimize the position error of the AUV simulation.

Ziegler-Nichols PID tuning method was used to find the suitable gain for the PID but the result yields more error rather than improvement. The error is due to that Ziegler-Nichols method gains only apply to the ideal, parallel form of the PID controller where the AUV simulation is non-ideal because all the disturbance the AUV will be facing in the real world are included. Table below shows the result for the Ziegler-Nichols method.

Table 4.2 shows the highlighted number are the benchmark results while green highlighted are Ziegler-Nichols method result.

			Position Error	Velocity Error
K_p	K_i	K_d	Avg	Avg
9	10	6	-0.0417	-0.0784
1.44	7.48	0.0693	-1.202	0.6563

The Ziegler-Nichols method produce proportional gain K_p , integral gain K_i , and derivative gain K_d , 1.44, 7.48 and 0.0693 respectively. The results of position error and the velocity error for the Ziegler-Nichols method is much larger than the benchmark result that is highlighted in yellow. This show that Ziegler-Nichols method is not suitable because the value for position error and the velocity error is increasing supposedly to minimize the error the value

of the average (avg) for position error and velocity error is smaller than the benchmark results. The negative sign represents the direction of the trajectory.

The gain (K_p , K_i and K_d) that produce from the Ziegler-Nichols method are adjusted to study the effect of each gain towards the Position Error and Velocity Error. Starting with the proportional gain, K_p is increase from 1 to 10 while the K_i and K_d value will be constant as 8 and 1 respectively. The value of 8 and 1 is the round-off value of the K_i and K_d gain from the Ziegler-Nichols method to change the decimal point to whole number. Table 4.3 below shows the result of the proportional gain, K_p is increase.

Table 4.3 show the result for position error and velocity error if K_p is increase.

Kp	Ki	Kd	Position Error	Velocity Error
			Avg	Avg
9	10	6	-0.0417	-0.0784
1.44	7.48	0.0693	-1.202	0.6563
1	8	1	0.1509	-1.0555
2	8	1	0.1053	-0.206
3	8	1	0.0731	-0.1191
4	8	1	-0.0679	-0.1716
5	8	1	0.0563	-0.2371
6	8	1	0.0551	-0.2897
7	8	1	0.0527	-0.3259
8	8	1	0.0582	-0.3616
9	8	1	0.0537	-0.4219
10	8	1	0.0728	-0.4088

As the K_p increase the average value for the Position Error will decrease slowly but at the same time the average of velocity error will increase. At higher K_p value the position error will be smaller while the average value of velocity error will be larger but when the K_p value higher than 10 the Position Error start to increase. Thus, we can reduce the position error by increase the value of K_p not more than 10 but velocity error will increase.

Next, the integral gain, K_i is increase to 13 starting from 1. Previously, K_p is only increase to 10 but for K_i it will be increase to 13 dues to the pattern is not really visible to analyze if the range is small. For this test the K_p and K_d value will constant as 6 and 1 respectively. The K_p value is set to 6 because from the previous test the value 6 has one of the lowest Position Error and Velocity Error.

Table 4.4 show the result of position error and velocity error if K_i is adjusted.

			Position Error	Velocity Error
K_p	K_i	K_d	Avg	Avg
9	10	6	-0.0417	-0.0784
1.44	7.48	0.0693	-1.202	0.6563
6	1	1	0.1118	-0.2828
6	2	1	0.1151	-0.2977
6	3	1	0.1485	-0.3279
6	4	1	0.1337	-0.2649
6	5	1	0.1642	-0.2635
6	6	1	0.1582	-0.278
6	7	1	0.0512	-0.2836
6	8	1	0.0551	-0.2897
6	9	1	0.0532	-0.2584
6	10	1	0.0561	-0.2653
6	11	1	0.1787	-0.2563
6	12	1	0.0619	-0.2569
6	13	1	0.0689	-0.267

The average of velocity error is decreased when the K_i value is increase but the position error average is fluctuating mean that it is not proportionally decrease or increase. At certain value of K_i such as 1 to 6 the position error is high but when at another value of K_i such as 7 to 10 the position error is low and at $K_i = 11$ the position error high again. This show that increasing the K_i value the velocity error can be reduced but to reduced position error K_i must be selected from range 7 to 10.

Lastly, the derivative gain, Kd is adjusted where the Ki value is constant as 12 because during the Ki test the Ki = 12 has the lowest velocity error while the position error is one of the lowest. The table below shows the result of the gain.

Table 4.5 shows the result of the error when Kd is increase.

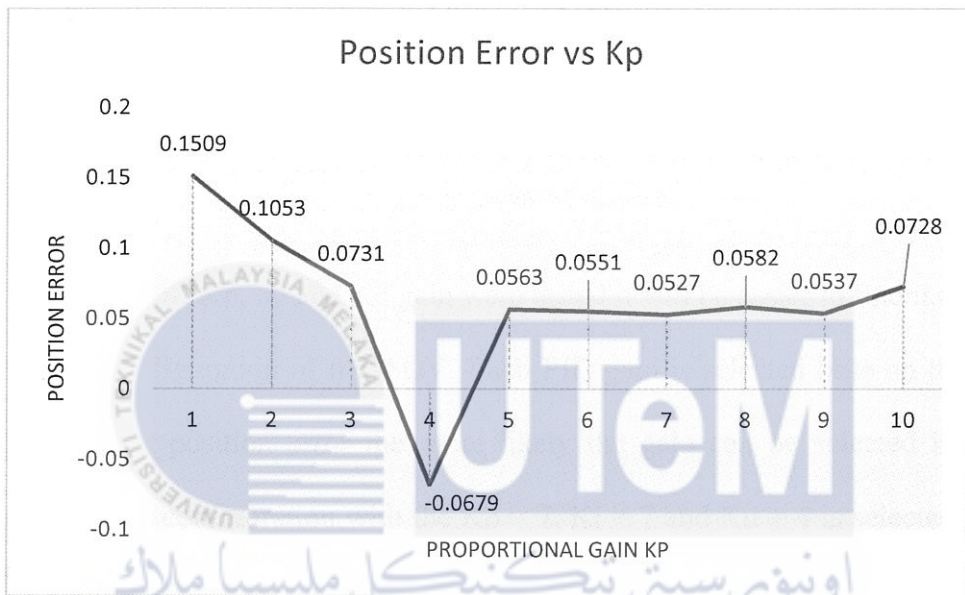
			Position Error	Velocity Error
Kp	Ki	Kd	Avg	Avg
9	10	6	-0.0417	-0.0784
1.44	7.48	0.0693	-1.202	0.6563
6	12	1	0.0619	-0.2567
6	12	2	0.1102	-0.1108
6	12	3	0.0544	-0.0736
6	12	4	-0.0122	-0.0873
6	12	5	0.0484	-0.1463
6	12	6	-0.0546	-0.0833
6	12	7	0.0634	-0.1281
6	12	8	-0.0577	-0.0848
6	12	9	-0.0213	-0.095
6	12	10	0.0763	-0.0948

The increasing value of Kd resulting the position error and velocity error to fluctuate above and below the benchmark result. For example, when Kd = 4 the position error is lesser than the benchmark result but when Kd = 6 the position error is larger than benchmark results. Even though the velocity error is rise if Kd value is increase but the different gap between the benchmark result is still lower when compare with the different gap of velocity error in Kp and Ki were tested.

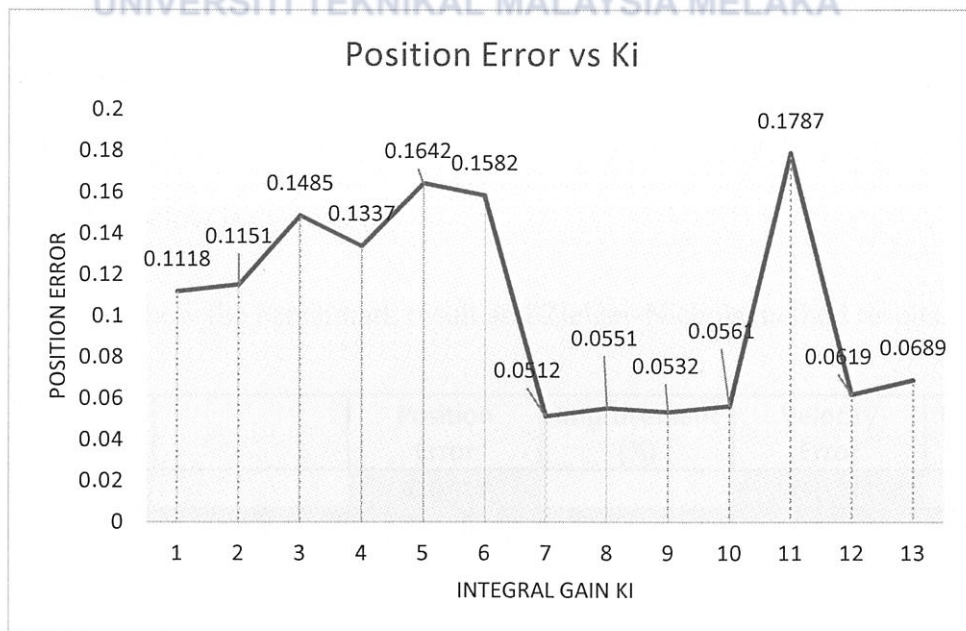
4.3 The Configuration of the Kp, Ki, and Kd Gain

The table in section 4.2 (The Effect of Kp, Ki and Kd) are plotted in graph to make a better understanding of it. This project concentrates more on how to reduce the position error rather than to reduce velocity error thus only the Position Error graph will be plotted.

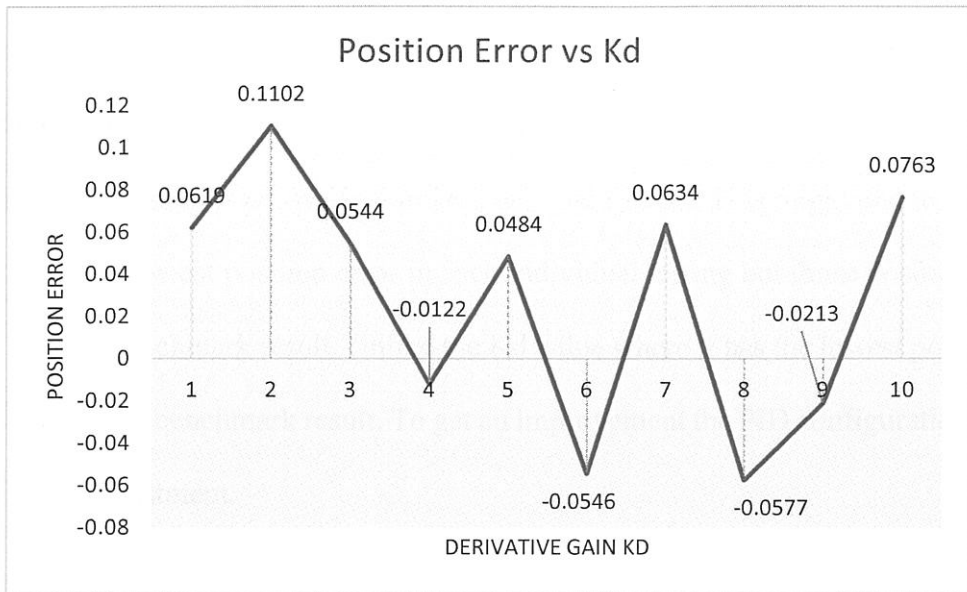
Graph 4.1 shows the result of Kp gain test.



Graph 4.2 shows the result of Ki gain test.



Graph 4.3 shows the result of Kd gain test.



After each of the K_p , K_i and K_d gain were tested it will be easier to find the best option for the PID gain configuration of the AUV. Each PID gain is selected base on their position error. The lesser the position error the more likely the gain can be selected into the PID configuration. A PID configuration with the $K_p = 7$, $K_i = 7$ and $K_d = 4$ is selected because in each of the gain testing those value have the lower position error. Refer to Graph 4.1 the $K_p = 7$ has lowest position error in Graph 4.2 $K_i = 7$ has the lowest position error and in Graph 4.3 $K_d = 4$ has the lowest position error. The PID configuration $K_p = 7$, $K_i = 7$ and $K_d = 4$ was given a simulation test to see whether the position error and velocity error will show any improvement. Table below is the result.

Table 4.6 show the benchmark result and Zielger-Nichols method results.

K_p	K_i	K_d		Position Error	Improvement (%)	Velocity Error	Improvement (%)
9	10	6		-0.0417		-0.0784	
7	7	4		-0.0552	-24%	-0.0956	-17%

The number that highlighted in yellow is the benchmark result while the green highlighted is the selected PID configuration. There is no improvement with the selected PID gain even though all the gain has the lowest position error during testing. This show that the selected PID configuration is not well optimized with the system. This might due to the Kp and Ki gain both has the lowest position error in each individual testing but those position errors is still larger than the benchmark result. Unlike the Kd value where it has the lowest position error and it is lower than the benchmark result. To get an improvement the PID configuration required to undergo a fine adjustment.

First, the Kp will be tuned by changing the Kp gain value to next lowest position error to see any improvement. Table below shows the result.

Table 4.6.1 show the result of tuning Kp gain.

Kp	Ki	Kd	Position Error	Improvement (%)	Velocity Error	Improvement (%)
9	10	6	-0.0417		-0.0784	
7	7	4	-0.0552	-24%	-0.0956	-17%
9	7	4	0.0203	51%	-0.0937	-16%
6	7	4	-0.0245	41%	-0.0807	-3%
5	7	4	-0.0605	-31%	-0.1042	-25%
8	7	4	0.0225	46%	-0.1091	-28%
4	7	4	-0.085	-51%	-0.1073	-27%

The Kp value is changed to 9 the second lowest position error during the Kp gain testing (refer graph 1) show improvement for the position error by 51% but the velocity error decrease by 17%. Next, the Kp is changed to another lowest position error until there is no improvement to be seen. The position error improves when Kp = 9, 6 and 8 but all of them didn't improve the velocity error.

Next, Ki value will be adjusted by the same method during the adjustment of the Kp.

Table below shows the result.

Table 4.6.2 show the result of tuning Ki gain.

Kp	Ki	Kd	Position Error	Improvement (%)	Velocity Error	Improvement (%)
9	10	6	-0.0417		-0.0784	
7	7	4	-0.0552	-24%	-0.0956	17%
7	9	4	-0.0528	21%	-0.0901	13%
7	8	4	-0.0398	5%	-0.0999	22%
7	10	4	-0.0314	25%	-0.0601	23%
7	1	4	0.0481	13%	-0.085	8%

By adjusting the value of Ki = 10 the position error and velocity error are managed to be improve by 25% and 23% respectively. At Ki = 8 the position error can be improved by 5% but the improvement of velocity error reduces by 22% which is quite large. Previously, when adjusting the Kp gain only the position error are improved by 56% which is larger than the improvement made by adjusting the Ki gain but it couldn't improve the velocity error as Ki did.

Lastly is the fine adjustment for the Kd value with same method as previous adjustment. Table below is the result of the tuning.

Table 4.6.3 show the result of tuning Kd gain.

Kp	Ki	Kd	Position Error	Improvement (%)	Velocity Error	Improvement (%)
9	10	6	-0.0417		-0.0784	
7	7	4	-0.0552	-24%	-0.0956	17%
7	7	9	0.0561	25%	-0.1047	25%
7	7	5	0.0294	29%	-0.0823	5%
7	7	12	-0.0901	54%	-0.0706	10%
7	7	11	0.0652	-34%	-0.0966	1%
7	7	6	-0.0183	56%	-0.0654	17%
7	7	8	0.0245	41%	-0.1028	24%
7	7	10	-0.0514	19%	-0.0889	12%

The tuning of the Kd value show an improvement at position error and velocity error. Some Kd value only improve the position error such as Kd = 5, 8 and some Kd value only improve velocity error at Kd = 10 but at Kd = 6 both position and velocity error are improved by 56% and 17%. Only by adjusting the Ki and Kd value both the position error and velocity error can be improved whereas adjusting Kp value only improve position error.

After all the Kp, Ki, and Kd gain value undergo fine adjustment, the gain that show improvement on the position error will be selected to test a new PID configuration. The gain that are chose are Kp = 9 (56% position error improvement), Ki = 10 (25% position error improvement) and lastly Kd = 8 (41% position error improvement). The new PID configuration is tested and the result as below.

Table 4.7 show the result of tuning Kp, Ki and Kd gain.

Kp	Ki	Kd	Position Error	Improvement (%)	Velocity Error	Improvement (%)
9	10	8	-0.0483	-14%	-0.0853	-8%

The new PID configuration fail to improve the position error and velocity error. This is due to the PID gain have been completely changed to a new value instead by adjusting one gain at a time. Thus, the new PID configuration require to undergo a new fine adjustment such as previous adjustment if want to improve the error.

4.4 AUV Simulation Output Results

In this section the output data from the AUV simulation is analyses. The output data is the AUV velocity and its position. In the previous section some of the PID configuration successfully improve the position and velocity error thus, only the output data of AUV that using those PID configuration will be taken.

4.4.1 Position Output Data

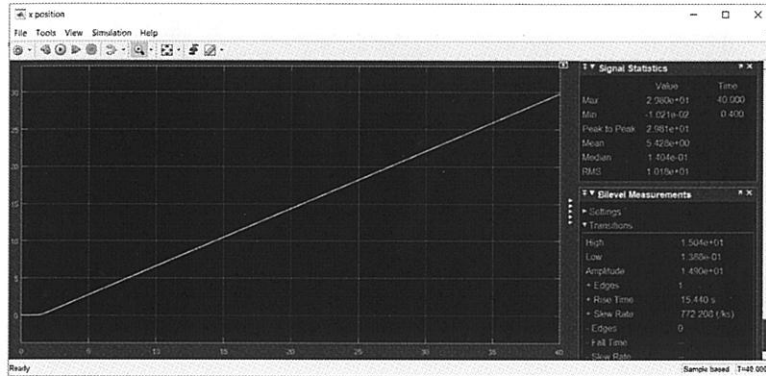


Figure 4.6: show the Position data for PID $K_p = 7$, $K_i = 10$, $K_d = 4$

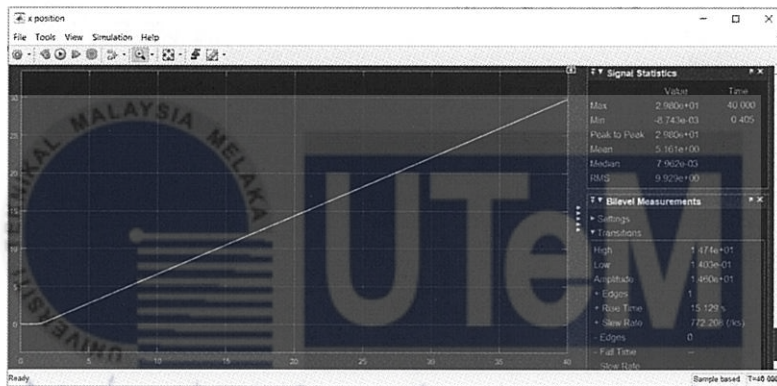


Figure 4.7: show the Position data for PID $K_p = 7$, $K_i = 7$, $K_d = 6$

The simulation is running for 40 second and within that time the AUV capable to reach 8m. From the figure above, both graph show that the AUV reach the same distance but have different rise time. AUV simulation with PID configuration $K_p = 7$, $K_i = 10$, $K_d = 4$ have the rise time 15.440 second while the PID configuration $K_p = 7$, $K_i = 7$, $K_d = 6$ have the rise time 15.129 second which is less time taken.

4.4.2 Velocity Output Data

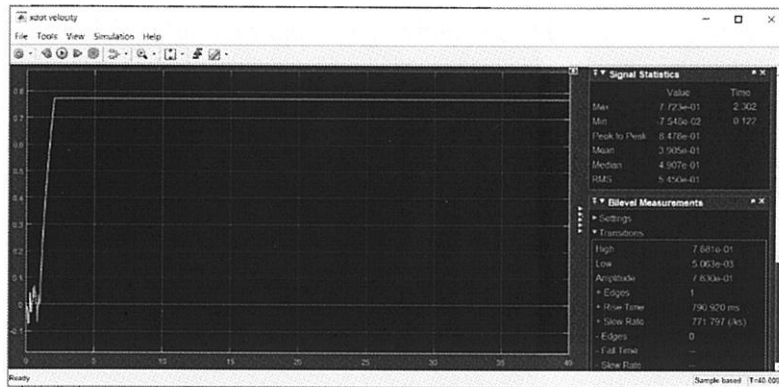


Figure 4.8: show the Velocity data for PID $K_p = 7$, $K_i = 10$ $K_d = 4$

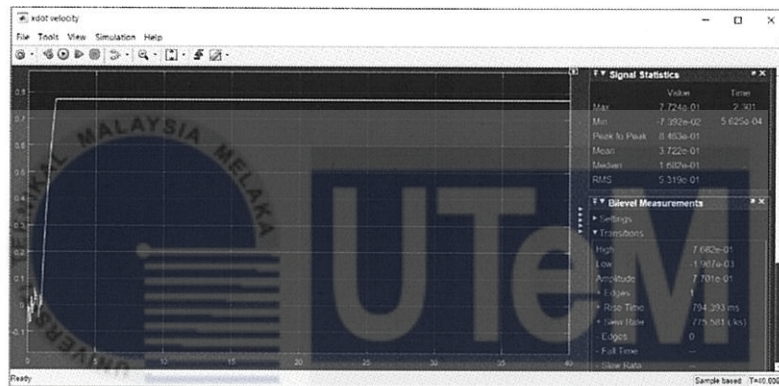


Figure 4.9: show the Velocity data for PID $K_p = 7$, $K_i = 7$, $K_d = 6$

The figure above both show the velocity data of the AUV simulation where both graphs have almost the same maximum amplitude and almost same time taken to reach the maximum amplitude which are 0.77 and 2.301 second respectively. The reference input for both graphs are 1 (one) but it can only achieve 0.77 this is due to the disturbance included in the simulation that is why there is decrement.

In figure 4.8 PID configuration $K_p = 7$, $K_i = 10$ $K_d = 4$ have a rise time of 794 ms while in figure 4.9 PID configuration $K_p = 7$, $K_i = 7$, $K_d = 6$ have a rise time of 790 ms. Mean that PID configuration in figure 4.8 take less time to reach maximum AUV velocity compare to PID configuration in figure 4.9. Even though the PID configuration in figure 4.8 reach maximum

velocity faster but it only can improve the position and velocity error lesser than PID configuration in figure 4.9. This can cause by when the AUV moving straight and the sensor has detected any deviation from its path the PID will try to bring back the AUV into its original path by decrease the speed of the AUV and when it returns to its original path the AUV will increase it speed again. That is why PID configuration in figure 4.9 take longer time to reach maximum velocity even though it improves the position and velocity error more than PID configuration in figure 4.8.



CHAPTER 5

CONCLUSION AND RECOMMENDATION

5.1 Conclusion

The effect of PID gain towards the AUV simulation are studied as shown in section 4.2 The Effect of K_p , K_i and K_d .

The gain value that have lowest position error during a test to study the effect of the PID towards the AUV simulation are selected and undergo a fine adjustment one gain at a time. First, the adjustment of K_p show that it only improves the position error while velocity error doesn't show any improvement. Secondly the adjustment of K_i gain and follow by K_d gain. Both gains improve the position error and velocity error but with a slightly different percentage of improvement. The tuning of K_i gain improves more on the velocity error while the tuning of K_d gain improve more on position error.

This project mainly focuses on how to reduce the position error, thus the tuning of K_d gain succeed to achieve the goal of the project.

As conclusion PID configuration $K_p = 7$, $K_i = 7$ and $K_d = 6$ offer the best PID configuration improvement for both position error and velocity error by 56% and 17%.

5.2 Recommendation

There're some suggestion or recommendation to improve this project which are the range of gain value that been selected to do a test on studying the effect of K_p , K_i and K_d towards the AUV can be double the current range which is from 1 to 10. This will give more data and accuracy to analysis the pattern of each gain.

Next, Ziegler-Nichols method fail to improve the position error and velocity error, thus used a different PID tuning method to find the best PID configuration such as Tyreus - Luyben method.



REFERENCES

- Mohd Shahrieel, M. A., Kasdirin, H. A., Jamaluddin, M. H. & Basar, M. F., 2009. Design and Development of an Autonomous Underwater Vehicle (AUV-FKEUTeM). pp. 1-3.
- Gonzalez, L. A., 2004. DESIGN, MODELLING AND CONTROL OF AN AUTONOMOUS UNDERWATER VEHICLE. *Bachelor of Engineering Honours Thesis*.
- Kennedy, J., 2002. Decoupled Modelling and Controller Design for the Hybrid Autonomous Underwater Vehicle: MACO.
- J.H.A.M, V., 2009. Modeling and Control of an Unmanned Underwater Vehicle. pp. 6-32.
- Bo, H. et al., 2013. A Fuzzy-PID Method to Improve the Depth Control of AUV. *IEEE International Conference on Mechatronics and Automation*, pp. 1528-1533.
- Mohd Aras, M. S. et al., 2017. Performance Analysis of PID and Fuzzy Logic Controller for Unmanned Underwater Vehicle for Depth Control. *Journal of Telecommunication, Electronic and Computer Engineering*, 9(3-2), pp. 59-60.
- G, I., 1998. Modelling and Identification of Underwater Robotics System. pp. 21-33.
- Thor, I. F., 1995. *Underwater Vehicle Dynamics*. Albuquerque: Book TSI Press.
- W, W. & C, M. C., 2001. Modelling and Simulation of the VideoRay Pro III Underwater Vehicle.